

EFFECTS OF TRANSPORT STRESS ON THE INTESTINES INVOLVING NEURONAL NITRIC OXIDE SYNTHASE

Jing LAN¹, Tonghui MA¹, Peng YIN², Kedao TENG¹, Yunfei MA (✉)¹

1 College of Veterinary Medicine, China Agricultural University, Beijing 100193, China.

2 School of Engineering Medicine, Beihang University, Beijing 100191, China.

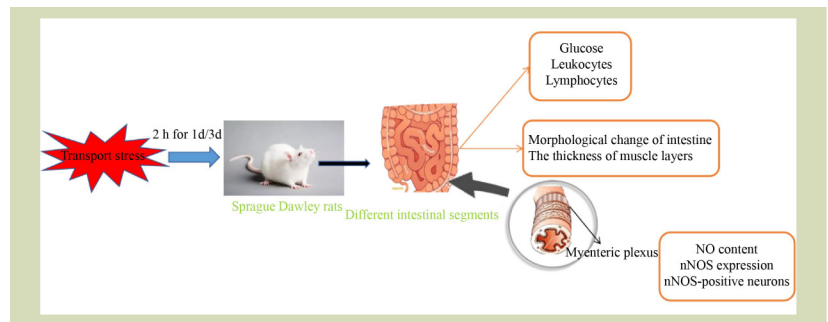
KEYWORDS

intestine, nNOS, nNOS-positive neurons, transport stress

HIGHLIGHTS

- Transport stress declined the level of leukocytes including lymphocytes in rat serum.
- Transport stress destroyed intestinal integrity of rat.
- The muscular layer thickness of intestine was decreased after transport stress.
- nNOS expression and nNOS-positive neurons were reduced in rat after transport stress.

GRAPHICAL ABSTRACT



ABSTRACT

Transport stress is commonly suffered by animals with gastrointestinal dysfunction a common symptom. Currently, the mechanisms of transport stress-induced intestine impairment are largely unknown. The aim of this study was to investigate the effects of transport stress on the expression of neuronal nitric oxide synthase (nNOS) and the distribution of nNOS-positive neurons of the intestines in rats and to explore the neuroendocrine mechanism of transport stress. In this study, Sprague Dawley rats ($n = 6$) were subjected on a constant temperature shaker for 1 (S1d) or 3 d (S3d). Rats exhibited increased serum glucose and diminished total number of leukocytes, in which lymphocytes level was also decreased in the S1d group ($P < 0.05$). Also, normal intestinal morphology was disrupted in the S1d rats, and the thickness of muscle layers was decreased in duodenum, jejunum and colon of S3d rats. In addition, it was found that nNOS expression, as well as the number of nNOS-positive neurons in the myenteric plexus were downregulated in duodenum, jejunum and colon of S3d rats compared with that of unstressed rats ($P < 0.05$). These data reveals that transport stress induced intestinal damage and uncovers potential action mechanisms that nNOS-positive neurons and nNOS expression might be involved in modulating this process.

Received August 13, 2022;

Accepted September 29, 2022.

Correspondence: yunfeima@cau.edu.cn

© The Author(s) 2022. Published by Higher Education Press. This is an open access article under the CC BY license (<http://creativecommons.org/licenses/by/4.0>)

1 INTRODUCTION

Animals are often exposed to transport stress because it is

related to a number of contributing factors, including crowding, temperature, noise and motion^[1]. Additionally, transport stress is a complex stress, in which many other

stressors are involved, for example, physical (including temperature, noise, motion, fasting, food and water deprivation) and social (including crowding and novel environment) challenges. This can result in weight loss, decreased conversion of feed into meat, increased physical injury and susceptibility to disease, tissue damage, attenuate immunity and even death^[2,3].

The intestinal mechanisms that respond to external stress signals are not fully understood. Although many studies have reported livestock transport stress, the effects of transport stress on the intestines are unclear. Nitric oxide is a major inhibitory neurotransmitter that mediates non-adrenergic and non-cholinergic inhibitory responses to stimulation^[4]. NO is generated from L-arginine by neuronal nitric oxide synthase (nNOS)^[5,6]. Evidence suggests that NO have a neuromodulator effect and act as a secondary messenger in the interstitial cells of Cajal and smooth muscle^[7,8]. Additionally, NO has inhibitory effects on the smooth muscle in some parts of the gut^[9]. A previous study reported that changes in the gastric motility of rats under stress was linked to changes in NO synthesis^[10]. Therefore, we hypothesized that nNOS-immunoreactive neurons and nNOS in the myenteric plexus are closely related to intestinal injury arising from transport stress.

Transport stress in the animal is one of the major concerns in the breeding industry and may be also considered as a model for subacute stress in humans. Therefore, it is of interest to investigate this subacute stress response induced by 1 or 3 d of road transport in the rats. Although many studies have reported livestock transport stress, the effects of transport stress on the intestines have not yet been explored. In this study, we used a simulated transport stress model to investigate the effects of transport stress on glucose, immune cell, intestinal morphology, and nNOS expression, as well as the distribution of nNOS-positive neurons in the duodenum, jejunum and colon of rats. The aims of this study were to evaluate the harmful effects of transport stress on the intestine, elucidate the potential mechanism of transport stress.

2 MATERIALS AND METHODS

2.1 Animal care and experimental groups

Thirty-six Sprague Dawley (SD) rats weighing 200 ± 10 g were supplied by the Beijing Vital River Laboratory Animal Technology Co., Ltd. (Beijing, China). Rats were kept at 25 ± 2 °C under a 12:12 h L:D photoperiod for 7 d to acclimate.

Animals had free access to water and food. On the eighth day, rats were randomly divided into the following three groups: control (CON), 1 d stress (S1d), 3 d stress (S3d). In each group, six rats were housed in plastic cages with a layer of wood shavings during the experiment. All cages were thoroughly cleaned and sterilized.

2.2 Transport stress models and animal treatment

A rat model of simulated transport stress was established as described previously^[11,12]. At the beginning of the experiment, SD rats in group CON were housed in a controlled environment, while rats in the transport stress groups were subjected to vibration at 30 ± 0.2 °C and $120 \text{ r}\cdot\text{min}^{-1}$ on a constant temperature shaker (DHZ-CA, Taicang Co., Ltd., Tianjin, China) from 8:00–10:00 every day to continuously simulate transport stress for 1 or 3 d. There were six rats in each group, and all results were acquired from three independent tests.

2.3 Sample collection

Rats in each group were anesthetized with 1% sodium pentobarbital (5 mg per 100 g bodyweight). Blood was collected from a jugular vein immediately after anesthesia, and then rats were sacrificed through neck dislocation. Blood was centrifuged to obtain serum samples for the analysis of glucose, as well as the number of leukocyte and lymphocyte. The intestines, including the duodenum, jejunum, and colon tissues, were excised, cut into 3-cm sections, placed in sample tubes, frozen in liquid nitrogen, and stored at -80 °C for subsequent experimentation, including enzyme-linked immunosorbent assay (ELISA), semiquantitative reverse transcription-polymerase chain reaction (RT-PCR). The six rats in each of the other groups were anesthetized with sodium pentobarbital, and then sections of the duodenum, jejunum, and colon were instantly removed and washed with physiological saline, cut into 2 cm blocks, and fixed with 10% buffered formalin phosphate for 48 h prior to paraffin embedding for morphological analysis. Intestine blocks were fastened with 4% (w/v) formaldehyde solution at 4 °C for 1 d. After overnight cryoprotection with 30% (w/v) sucrose in PBS, the blocks were embedded and cut into 30- μm -thick sections using a freezing microtome to perform immunohistochemical and immunofluorescence staining.

2.4 Biochemical indicator analysis

Concentrations of serum glucose were detected by an automated biochemical analyzer (TBA-40FR, Toshiba, Tokyo,

Japan), in which the glucose oxidase method was used for glucose. Numbers of leukocyte and lymphocyte were counted by an automated blood cell analyzer (Mek-7222K, Nihon Konden, Tokyo, Japan) with electric-resistivity method.

2.5 Histopathological assay

Samples were embedded in paraffin, and then sectioned (5 μm). Sections were stained with hematoxylin and eosin (H&E) immediately after dewaxing and dehydration. The intestinal morphology and thickness of muscle layers were observed and photographed under a Nikon B80i microscope (Nikon, Tokyo, Japan) by image capturing software. Three slices were randomly selected from each animal, and the thickness of muscle layers was determined at 10 measuring points using a light microscope under a 4X microscope (Olympus IX70, Olympus Corporation, Beijing, China) combined with Leica software (Leica Application Suite, version 2.8.1, Leica Microsystems, Wetzlar, Germany), for which five representative fields of view were captured and five positions from each field were selected for measuring the thickness of the muscular layers.

2.6 Immunohistochemistry for nNOS

To avoid endogenous peroxidase reactivity, frozen sections were incubated in 2% hydrogen peroxide for 15 min after washing with PBS. All incubations were conducted at room temperature and slices were rinsed in PBS including 0.3% Triton X-100 (PBS-X). Sections were incubated in the primary antibody, polyclonal antibody, which was raised in sheep against nNOS (1:1000; ab1529, Millipore, Billerica, MA, USA) for 24 h at 4 °C, then rinsed with PBS (0.15 mol·L⁻¹) and interacted with biotinylated donkey anti-sheep IgG (1:100; 711067003, Jackson ImmunoResearch Laboratories, West Grove, PA, USA) in PBS-XCD for 2 h. Next, the sections were placed in ABC-peroxidase solution (1:100; PK-6102, Vector, Torrance, CA, USA) for 30 min and the bound peroxidase eventually formed a brown reaction product by reacting with 0.02% diaminobenzidine-4HCl (DAB; D5637, Sigma Chemical Co., St. Louis, MO, USA) and 0.0001% H₂O₂ in 50 mmol·L⁻¹ Tris-HCl (pH = 7.6). All sections were fixed to gelatinized slides, dried, dehydrated in graded ethanol, rinsed in xylene, and covered with coverslips. The quantity of nNOS-immunoreactive cells in the myenteric plexus was observed under a microscope (Ni-U, Nikon, Tokyo, Japan). Stained slides were imaged using a light microscope with images input through a solid-state camera to the microcomputer-based

imaging system. At least five myenteric plexus ganglia per animal were counted for the total number of nNOS-immunoreactive cells. Positivity was defined by the presence of a dark immunoreaction product in the neuronal cell body. The nuclei of the neurons did not immunolabel and were observed as clear areas. Both positive and negative cell bodies were counted, and the nNOS-positive neurons were expressed as a percentage of the total number of neurons. The percentage of nNOS-positive neurons per ganglia was calculated and averaged for each site (duodenum, ileum and colon) for each rat.

2.7 Determination of nNOS levels by ELISA

Intestine segments were homogenized with 0.9% saline (1:9) on ice, and then centrifugated at 1000 × g for 10 min to obtain the supernatant. Concentrations of nNOS in different intestinal segments were determined using commercially available ELISA kits (Xitang Biotech Co., Ltd., Shanghai, China) following the manufacturer's instructions. Finally, the nNOS contents were quantified using a microplate reader, and the absorbance was measured at 450 nm.

2.8 RNA isolation and RT-PCR

RNA extraction and RT-PCR were conducted following previously described methods^[13]. Total RNA was extracted by TRIzol reagent (Invitrogen, Carlsbad, CA, USA), and then purified with a RNeasy mini kit (Qiagen, Valencia, CA, USA) following the manufacturer's instructions. The quality of the purified RNA was evaluated by computing the ratio of the absorbance at 260 and 280 nm using a NanoDrop ND-1000 spectrophotometer (NanoDrop Technologies, Wilmington, DE, USA). Next, purified RNA was reverse transcribed to cDNA using a FastQuant RT kit (Tiangen Biotech Co., Ltd., Beijing, China). Finally, nNOS mRNA expression was quantified by RT-PCR. Glyceraldehyde-3-phosphate dehydrogenase (GAPDH) was used as the reference gene. The primer sequences of the nNOS and GAPDH genes used in this study are as follows: nNOS-forward: 5'-GCCGTAACAAAG GAAATAGAAACA-3'; nNOS-reverse: 5'-TGGTCACCTCCA GCACAAGAT-3'; GAPDH-forward: 5'-CAACATCCATGA CAACTTTG-3'; GAPDH-reverse: 5'-GTCCACCACCCTGT-TGCTGTAG-3'. The cycling parameters used for amplification were as follows: initial heat denaturation at 95 °C for 5 min; 30 cycles at 94 °C for 5 min, 55 °C for 45 s, and 72 °C for 30 s; and a final extension at 72 °C for 7 min.

2.9 Data analysis and statistics

There were six rats in each group, and the results were acquired as the means of three independent experiments. Values are expressed as the mean \pm SEM. The data were evaluated by a one-way analysis of variance with post-hoc multiple comparison testing using Tukey's (for comparison of each group to every other group) or Dunnett's (for comparison of each group to the control group) method utilizing SPSS v17.0 (SPSS Inc., Chicago, IL, USA). A threshold of $P < 0.05$ was considered statistically significant.

3 RESULTS

3.1 Transport stress enhances glucose content in the rats

To assess the intestinal stress response of rats following simulated transport, we determined the content of plasma glucose in the rats from each group, which was significantly affected by transport time ($P < 0.05$). As shown in Fig. 1, the

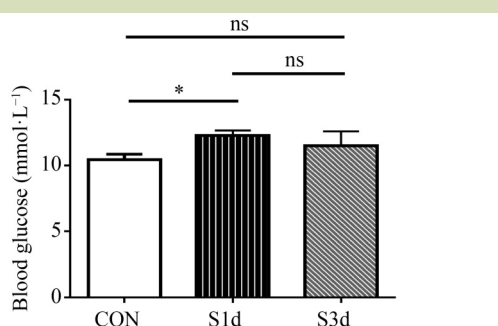


Fig. 1 Transport-associated treatments induced changes in serum glucose levels. CON, control group; S1d, 1-d stress group; S3d, 3-d stress group. Values are presented as the mean \pm SEM ($n = 6$ rats for each group); * $P < 0.05$; ns, no significant difference. The data was expressed as the means of three independent experiments.

concentration of glucose in the S1d group was higher than the CON group ($P < 0.05$). There was an initial increase in glucose (1 d stress) and subsequent decrease (3 d stress), but there was not significant difference in glucose concentration between the CON and S3d groups (Table 1).

3.2 Transport stress decreases the number of leukocytes and lymphocytes in the serum

The production of leukocytes and lymphocytes is affected by many different stressors (Fig. 2). In the present study, the total mean numbers of leukocytes and lymphocytes decreased in the S1d group ($P < 0.05$) compared to the CON group, while the numbers in the S3d group almost recovered and were maintained at a similar level as the CON group (Table 1).

3.3 Histological changes in the intestines following simulated transport stress

To investigate the degree of intestinal tissue damage caused by simulated transport stress, dissection of the abdominal cavity of rats in the S1d group showed obvious hyperemia, hemorrhaging and inflation in the intestines (Fig. 3(a)).

Histopathological examination is considered a standard technique for analyzing morphological changes in different tissues. Figure 3(b) shows H&E-stained sections of the jejunum. Intestinal villi were integrated structurally in the CON group and normal intestinal cells were regularly and tightly arranged with clear structures. In the S1d group, intestinal villi were lost and villus integrity was damaged with desquamation observed at the tips of the intestinal villi and exposure of the lamina propria. Also, lesions were observed in interstitial edema, widespread gland cells were loosely arranged, inflammatory cells had infiltration and serious hemorrhaging was observed. Although the S3d group had blood vessels with obvious congestion, vasodilation and deformation, and there was inflammatory cell infiltration in the lamina propria, impairment of the intestinal mucosa was

Table 1 Changes in blood biochemical indexes

Group	Leukocytes ($\times 10^9 L^{-1}$)	Lymphocytes ($\times 10^9 L^{-1}$)	Glucose (mmol·L ⁻¹)
CON	16.91 \pm 2.02 ^a	12.25 \pm 1.21 ^a	10.44 \pm 0.43 ^a
S1d	7.97 \pm 1.35 ^b	5.97 \pm 0.57 ^b	12.29 \pm 0.39 ^b
S3d	14.27 \pm 1.76 ^a	11.53 \pm 1.21 ^a	11.51 \pm 1.10 ^a

Note: Data are mean \pm SEM ($n = 6$). Means followed by the same letter within columns are not significantly different at $P < 0.05$. CON, control group; S1d, 1-d stress group; S3d, 3-d stress group.

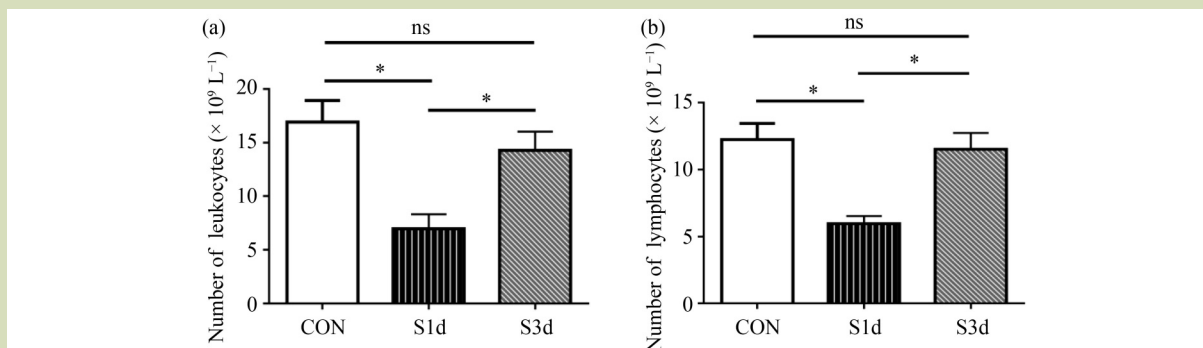


Fig. 2 The mean total number ($\times 10^9 L^{-1}$) of leukocytes (a) and lymphocytes (b) in the blood. CON, control group; S1d, 1-d stress group; S3d, 3-d stress group. Values are presented as the mean \pm SEM ($n = 6$ rats for each group); $*P < 0.05$; ns, no significant difference. The data was expressed as the means of three independent experiments.

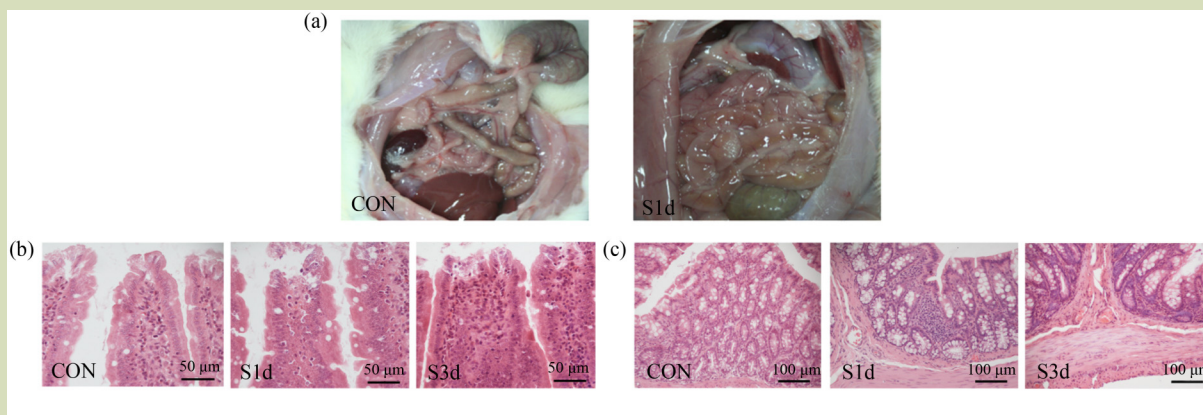


Fig. 3 Morphological changes of intestinal tissues following simulated transport stress. Pictures of dissected abdominal cavities of rats from the control and 1 d stress groups (a). Morphological changes in the intestinal tissues were measured using H&E staining and observed under an optical microscope for microstructures in the jejunum (b) and colon (c). CON, control group; S1d, 1-d stress group; S3d, 3-d stress group. Values are presented as the mean \pm SEM ($n = 6$ rats for each group).

relatively alleviated with less villus edges revealing slighter impairment than in the S1d group. Histopathological observation revealed the same results in the duodenum and jejunum. The colon histological analysis showed that the colon sections of the CON group were normal with structural integrity, and that transport stress induced less damage to the colon, which had several lymphocytes. These results are illustrated in Fig. 3(c).

3.4 Transport stress decreased muscular layer thickness of the intestines

Muscle layers reflect the intensities of intestine contractions; therefore, we investigated the influence of stress on muscle layers in duodenum, jejunum and colon. The muscle layer

analysis demonstrated that, when compared to the CON group, no significant effects on the duodenum were observed in the S1d group. However, the thickness of the muscle layers in the S3d group were reduced ($P < 0.05$) (Fig. 4(a)). Figure 4(b) shows that the stress treatment markedly reduced the muscle layer of the jejunum in both the S1d and S3d groups ($P < 0.05$). Next, we investigated changes in the thickness of the colon muscle layers (Fig. 4(c)). Our results indicated that S1d treatment enhanced the thickness of the muscle layers in the colon ($P < 0.05$). However, the thickness of the muscle layer dramatically declined in the S3d group ($P < 0.05$) compared with those in the CON group. In summary, the above results indicated that the thickness of the intestinal muscle layers was susceptible to S3d treatment and exhibited decreased thickness.

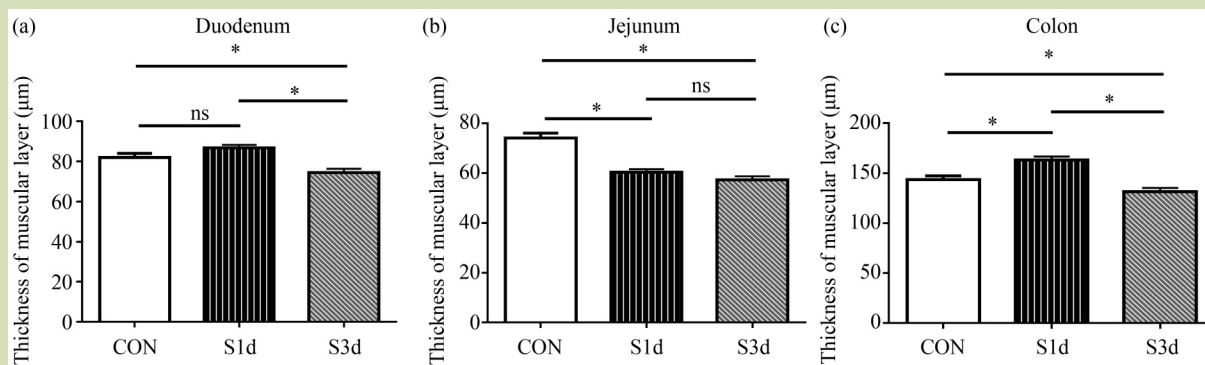


Fig. 4 The thickness of intestinal muscle layers was analyzed under a microscope. CON, control group; S1d, 1-d stress group; S3d, 3-d stress group. Values are presented as the mean ± SEM (*n* = 6 rats for each group); **P* < 0.05; ns, no significant difference. The data was expressed as the means of three independent experiments.

3.5 Transport stress declines nNOS content of the intestines

ELISA results revealed that compared with that of the CON group, S3d treatment significantly decreased the content of nNOS in the duodenum (*P* < 0.05) (Fig. 5(a)). We observe no clear sign of nNOS level in the S1d group relative to the CON group. As shown in Fig. 5(b), no significant difference was observed in the nNOS content between the S1d and CON groups in the jejunum, and when compared to the CON group, S3d treatment dramatically suppressed the level of nNOS in the jejunum (*P* < 0.05). Based on the results of ELISA, the content of nNOS in the colon of S3d group was significantly inhibited (*P* < 0.05) relative to the C group (Fig. 5(c)).

3.6 Transport stress declines nNOS mRNA expression in the intestines

We examined the expression of nNOS genes in the duodenum

by RT-PCR and found that nNOS mRNA expression was inhibited both in the S3d group when compared to the CON group (*P* < 0.05) (Fig. 6(a)). We also investigated the mRNA levels of nNOS in the jejunum. There was no evidence to indicate that there were changes in the nNOS mRNA levels of the S1d groups. Unlike the S1d group, the S3d treatment significantly affected and decreased the nNOS mRNA levels (*P* < 0.05) when compared to the CON group (Fig. 6(b)). There were no obvious changes between the S1d and CON groups in the colon. S3d treatment rarely affected nNOS mRNA expression when compared to the CON group (Fig. 6(c)).

3.7 Distribution of nNOS-positive neurons in the intestines

After transport stress simulation, we evaluated the locations of nNOS generated from nNOS-positive neurons in the intestines using immunohistochemistry assays. As shown in Fig. 7(a),

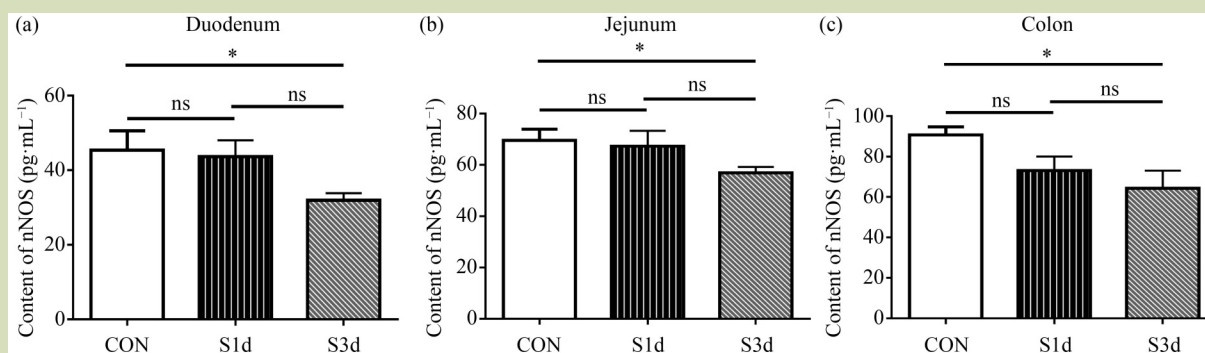


Fig. 5 The nNOS content of the intestines were detected by ELISA. CON, control group; S1d, 1-d stress group; S3d, 3-d stress group. Values are presented as the mean ± SEM (*n* = 6 rats for each group); **P* < 0.05; ns, no significant difference. The data was expressed as the means of three independent experiments.

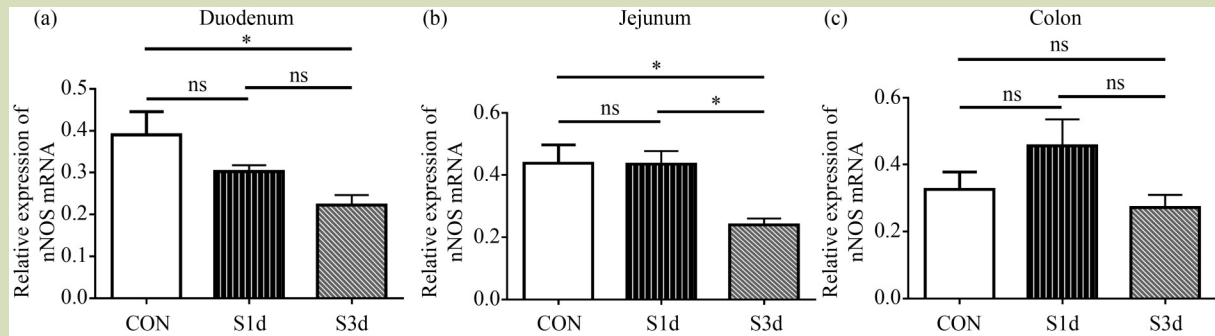


Fig. 6 Expression of nNOS mRNA in the duodenum (a), jejunum (b), and colon (c). CON, control group; S1d, 1-d stress group; S3d, 3-d stress group. Values are presented as the mean \pm SEM ($n = 6$ rats for each group); * $P < 0.05$; no significant difference. The data was expressed as the means of three independent experiments.

nNOS-positive neurons were mainly distributed throughout the myenteric plexus, and nNOS-immunoreactive staining was detected in the cytoplasm instead of the nucleus. The number of nNOS-immunoreactive neuronal cells was the greatest in the colon and smallest in the duodenum. Also, we recorded the number of nNOS-positive neurons in the myenteric plexus of three intestine sections under a microscope (Fig. 7(b)). No significant difference was observed in the number of nNOS-immunoreactive neurons in the S1d group in the jejunum. However, transport stress for 3 d resulted in reduced nNOS-immunoreactive neurons ($P < 0.05$) in the jejunum relative to the CON group.

4 DISCUSSION

The hypothalamic-pituitary-adrenal (HPA) axis is an important part of the neuroendocrine system and participates in regulating many physical activities^[12]. Recently, the HPA axis was found to react with the mechanisms of maintaining homeostasis that control stress responses^[14]. Specifically, HPA activation in stressful situations stimulates glucocorticoid secretion, which is extensively regarded as physiological performance under acute stress^[15], and triggers secondary responses associated with energy metabolism involving enhanced glucose levels and transformed electrolyte homeostasis^[16]. In our experiment, the data clearly revealed that when compared to the C group, rats in the stress groups exhibited increased serum glucose concentrations, suggesting that the HPA system was activated and responded to stress signals. Accordingly, the transport stress model was successfully established in this study. However, continuous treatment inhibited glucose levels in the S3d group when compared to the S1d group, which may be a result of elevated negative feedback from the HPA axis initiated by

corticosterone-sensitive target cells. We inferred the HPA system gradually adapted to stimuli after rats were exposed to constant stress, which repressed stress responses, mainly due to glucocorticoids, and decreased glucose concentrations according to previous research^[17]. In the present study, this process was responsible for the initial increase in glucose (1 d stress) and its subsequent decline (3 d stress).

A previous study showed that transport stress affects animal immune ability^[18]. In this study, both leukocytes and lymphocytes in the peripheral blood of the S1d group decreased markedly, demonstrating that transport stress resulted in immune containment. Obernier^[19] reported that continuous transport stress caused an immune suppression in peripheral blood. Consistent with the results of our work, both leukocyte and lymphocyte of peripheral blood in S2d and S3d group were significantly decreased^[20]. The marked decline in lymphocytes during transport elevated the plasma cortisol concentration^[21], however, plasma cortisol concentrations were not determined in the present study. Nevertheless, the effects of transport stress on lymphocytes numbers in this study is consistent with the findings of Dalin^[22], who found that the mean number of lymphocytes decreased markedly following transport stress. Notably, in our experiment, the total numbers of leukocytes and lymphocytes were lower following transport stress for 1 d than for 3 d, indicating that rats may undergo stronger pressure at the start of transport, adapt to disadvantageous situations during transport, and then return to normal immune functioning. Based on the data, we concluded that simulated transport stress led to a strong stress response and immunity effect, especially in the S1d group. Thereby, these results showed that rats may experience heightened stress at the beginning of transport, and then adapt to the perceived adverse environment later during transport,

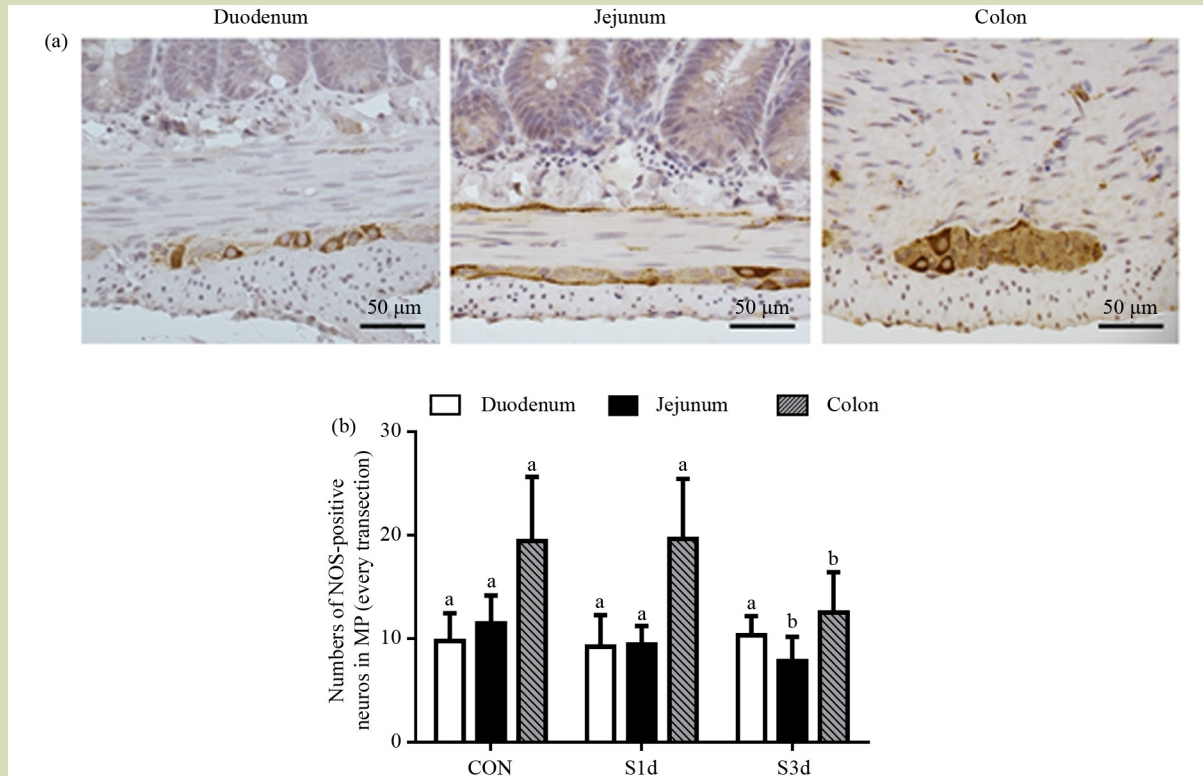


Fig. 7 The distribution of nNOS-positive neurons in the duodenum, jejunum, and colon. Images of nNOS immunohistochemistry staining in the intestines (a). Localization of nNOS-positive neurons by immunofluorescence staining (b). CON, control group; S1d, 1-d stress group; S3d, 3-d stress group. Values are presented as the mean \pm SEM ($n = 6$ rats per group); Different letters indicate that the changes between each group were statistically significant ($P < 0.05$). The data was expressed as the means of three independent experiments.

after which, they gradually return to normal physiological condition.

Activation of the HPA system caused by stress subsequently induced a reduction of intestinal blood flow, and thus hemorrhage, ischemia and degeneration of the intestinal mucosa^[23]. A previous study reported that following simulated transport stress, the rat jejunum was impaired^[11]. In the present study, following 1 d of transport stress, intestinal impairment was induced. For example, mucosal edema, bleeding and epithelial cells were shed from the villi, which usually emerge at the beginning of ischemia, per the findings of a previous study^[24]. In this study, the H&E results of the S1d group showed that there was more intestinal damage. Also, intestine microvillus height became shorter and sparser and intestinal epithelial cells shed, permeability increased, which then augmented inflammatory and immune responses to infection which was consistent with our results^[25]. However, stress did not affect colon morphology. In comparison to the S1d group, pathological changes in the S3d group were reduced as the result of repair and renewal of the rat intestine, which

may be due to the animal's ability to maintain homeostatic balance. Clearly, transportation treatment elicited a stress response, intestinal damage and disturbances, which were especially obvious in the S1d group. Also, the thickness of muscular layer of intestine was found to have decreased following simulated transport stress in our study, which indicated potential intestinal injury. Guo et al.^[26] suggested that decreased thickness of muscular layer of intestine reflects ongoing intestinal damage, which probably contributed to the pathological changes of intestine. Our HE staining confirmed the occurrence of intestinal damage.

Gastrointestinal (GI) function is regulated by the enteric nervous system. To uncover the underlying nervous mechanisms of transport-induced stress, the current study investigated the effects of transport stress on nNOS expression, and the distribution of nNOS-immunoreactive neurons in the myenteric plexus of the intestines in rats. The activity of GI smooth muscle cells is regulated by contractile cholinergic neurons and relaxant non-adrenergic, non-cholinergic (NANC) neurons in the myenteric plexus^[27]. The decline or

elevation of NANC relaxation may be responsible for the pathophysiology of dysfunctional GI tract motility. NO functions as an inhibitory NANC neurotransmitter in the enteric nervous system and exhibits various effects, such as acting as an intracellular secondary messenger and intercellular messenger^[8,28]. NO has essential physiological functions in many areas of the GI tract and is synthesized and secreted by reacting to nerve stimulation of the myenteric plexus, which thereby relaxes the smooth muscle in the intestines^[29]. The distribution of nNOS, which is an enzyme involved in NO synthesis through L-arginine, and the lack of this crucial enzyme combined with the disorder of local NO production may account for the defective relaxation of the GI tract^[30]. The presence of nitric oxide synthase (NOS) reflects the potential for NO synthesis and is found in neurons in the myenteric plexus. As described in previous research, knock out of nNOS exacerbates intestinal ischemia/reperfusion injury in mice^[31]. The decline of nNOS expression is related to impaired NO synthesis, which may account for intestinal dysmotility. Alternations of NOS synthesis in the gastric myenteric plexus may be connected to transcriptional, translational or posttranslational events. In this study, we analyzed the mRNA expression of nNOS through RT-PCR and at the protein-level through ELISA. We found that the effects of stress on the reduction of intestinal nNOS were more obvious following 3 d of transport stress, which is also consistent with the results of muscle layers thickness. In addition, nNOS immunoreactive neurons acted as inhibitory motor neurons, and was derived

from the myenteric plexus rather than the submucosal plexus in the colon^[32]. There is increasing evidence that the defective functioning of nNOS neurons in the myenteric plexus can lead to GI diseases^[30]. It was reported that the decreased density of nitregeric innervation is associated with several intestinal diseases, indicating that a lack of NO may be involved in impaired smooth muscle relaxation that is observed in these disorders^[33]. This study demonstrated that the number of nNOS neurons in the myenteric plexus was effectively suppressed following transport stress, particularly in the S3d group, and the density of nNOS neurons in the myenteric plexus of different tissues was weakened with reduced the thickness of muscle layers. Similarly, it was reported that decreased NO synthesis causes the contraction of smooth muscle and declines the thickness of muscle layers^[34].

5 CONCLUSIONS

In conclusion, transport stress affects immune function and intestinal integrity with the decline of muscle layer thickness. The results from the *in vivo* experiments presented here provide the evidence that the downregulation of nNOS level derived from nNOS-positive neurons in the myenteric plexus is related to transport stress, which was evidently observed in the S3d group compared to S1d group. The different effects of stress on the nNOS expression of the intestines may be related to distinct intestinal functions.

Acknowledgements

This work was supported by the National Natural Science Foundation of China (31772686 and 31502025) and the National Twelve-Five Technological Supported Plan of China (2011BAD34B01).

Compliance with ethics guidelines

Jing Lan, Tonghui Ma, Peng Yin, Kedao Teng, and Yunfei Ma declare that they have no conflicts of interest or financial conflicts to disclose. All applicable institutional and national guidelines for the care and use of animals were followed. The protocols used in this study conformed to the Guide to Laboratory Animals developed by the Ministry of Science and Technology. All procedures involving animals were approved by the Committee for the Care and Use of Experimental Animals, China Agricultural University (Beijing, China).

REFERENCES

1. He Y, Sang Z, Zhuo Y, Wang X, Guo Z, He L, Zeng C, Dai H. Transport stress induces pig jejunum tissue oxidative damage and results in autophagy/mitophagy activation. *Journal of Animal Physiology and Animal Nutrition*, 2019, **103**(5): 1521–1529
2. Ge J, Li H, Sun F, Li X N, Lin J, Xia J, Zhang C, Li J L. Transport stress-induced cerebrum oxidative stress is not mitigated by activating the Nrf2 antioxidant defense response in newly hatched chicks. *Journal of Animal Science*, 2017, **95**(7): 2871–2878
3. Li Z Y, Lin J, Sun F, Li H, Xia J, Li X N, Ge J, Zhang C, Li J L. Transport stress induces weight loss and heart injury in chicks:

- disruption of ionic homeostasis via modulating ion transporting ATPases. *Oncotarget*, 2017, **8**(15): 24142–24153
4. Gaynullina D K, Schubert R, Tarasova O S. Changes in endothelial nitric oxide production in systemic vessels during early ontogenesis—A key mechanism for the perinatal adaptation of the circulatory system. *International Journal of Molecular Sciences*, 2019, **20**(6): 1421
 5. Böger R, Hannemann J. Dual role of the L-arginine-ADMA-NO pathway in systemic hypoxic vasodilation and pulmonary hypoxic vasoconstriction. *Pulmonary Circulation*, 2020, **10**(S1): 23–30
 6. Vanhoutte P M, Zhao Y, Xu A, Leung S W S. Thirty years of saying NO: sources, fate, actions, and misfortunes of the endothelium-derived vasodilator mediator. *Circulation Research*, 2016, **119**(2): 375–396
 7. Huber A, Saur D, Kurjak M, Schusdziarra V, Allescher H D. Characterization and splice variants of neuronal nitric oxide synthase in rat small intestine. *American Journal of Physiology*, 1998, **275**(5): G1146–G1156
 8. Saur D, Neuhuber W L, Gengenbach B, Huber A, Schusdziarra V, Allescher H D. Site-specific gene expression of nNOS variants in distinct functional regions of rat gastrointestinal tract. *American Journal of Physiology. Gastrointestinal and Liver Physiology*, 2002, **282**(2): G349–G358
 9. Toda N, Herman A G. Gastrointestinal function regulation by nitrenergic efferent nerves. *Pharmacological Reviews*, 2005, **57**(3): 315–338
 10. Wrzos H F, Cruz A, Polavarapu R, Shearer D, Ouyang A. Nitric oxide synthase (NOS) expression in the myenteric plexus of streptozotocin-diabetic rats. *Digestive Diseases and Sciences*, 1997, **42**(10): 2106–2110
 11. Wan C, Yin P, Xu X, Liu M, He S, Song S, Liu F, Xu J. Effect of simulated transport stress on the rat small intestine: a morphological and gene expression study. *Research in Veterinary Science*, 2014, **96**(2): 355–364
 12. Wang L, Han D, Yin P, Teng K, Xu J, Ma Y. Decreased tryptophan hydroxylase 2 mRNA and protein expression, decreased brain serotonin concentrations, and anxiety-like behavioral changes in a rat model of simulated transport stress. *Stress*, 2019, **22**(6): 707–717
 13. Wang J, Li J, Yu M, Wang Y, Ma Y. An enhanced expression of hypothalamic neuronal nitric oxide synthase in a rat model of simulated transport stress. *BMC Veterinary Research*, 2019, **15**(1): 323
 14. Fazio E, Medica P, Cravana C, Ferlazzo A A. Pituitary-adrenocortical adjustments to transport stress in horses with previous different handling and transport conditions. *Veterinary World*, 2016, **9**(8): 856–861
 15. Goddard P J, Keay G, Grigor P N. Lactate dehydrogenase quantification and isoenzyme distribution in physiological response to stress in red deer (*Cervus elaphus*). *Research in Veterinary Science*, 1997, **63**(2): 119–122
 16. Ali B H, Al-Qarawi A A, Mousa H M. Stress associated with road transportation in desert sheep and goats, and the effect of pretreatment with xylazine or sodium betaine. *Research in Veterinary Science*, 2006, **80**(3): 343–348
 17. Makino S, Hashimoto K, Gold P W. Multiple feedback mechanisms activating corticotropin-releasing hormone system in the brain during stress. *Pharmacology, Biochemistry, and Behavior*, 2002, **73**(1): 147–158
 18. Zhang L, Yue H Y, Zhang H J, Xu L, Wu S G, Yan H J, Gong Y S, Qi G H. Transport stress in broilers: I. Blood metabolism, glycolytic potential, and meat quality. *Poultry Science*, 2009, **88**(10): 2033–2041
 19. Obernier J A, Baldwin R L. Establishing an appropriate period of acclimatization following transportation of laboratory animals. *ILAR Journal*, 2006, **47**(4): 364–369
 20. Wan C R, Ma W R, Yin P, Xu X L, Liu F H, Xu J Q. Effect of intestinal mucosal immunity induced by transport stress and the regulation mechanism of Suanzaoren decoction. *Journal of Chemical and Pharmaceutical Research*, 2013, **5**(11): 58–63
 21. Fauci A S. Immunosuppressive and anti-inflammatory effects of glucocorticoids. *Monographs on Endocrinology*, 1979, **12**: 449–465
 22. Dalin A M, Magnusson U, Häggendal J, Nyberg L. The effect of transport stress on plasma levels of catecholamines, cortisol, corticosteroid-binding globulin, blood cell count, and lymphocyte proliferation in pigs. *Acta Veterinaria Scandinavica*, 1993, **34**(1): 59–68
 23. Kuge T, Greenwood-Van Meerveld B, Sokabe M. Stress-induced breakdown of intestinal barrier function in the rat: reversal by wood creosote. *Life Sciences*, 2006, **79**(9): 913–918
 24. Yucel A F, Kanter M, Pergel A, Erbogga M, Guzel A. The role of curcumin on intestinal oxidative stress, cell proliferation and apoptosis after ischemia/reperfusion injury in rats. *Journal of Molecular Histology*, 2011, **42**(6): 579–587
 25. Collins S M. Stress and the Gastrointestinal Tract IV. Modulation of intestinal inflammation by stress: basic mechanisms and clinical relevance. *American Journal of Physiology. Gastrointestinal and Liver Physiology*, 2001, **280**(3): G315–G318
 26. Guo Y, Wang Q, Zhang K, An T, Shi P, Li Z, Duan W, Li C. HO-1 induction in motor cortex and intestinal dysfunction in TDP-43 A315T transgenic mice. *Brain Research*, 2012, **1460**: 88–95
 27. Van Geldre L A, Lefebvre R A. Interaction of NO and VIP in gastrointestinal smooth muscle relaxation. *Current Pharmaceutical Design*, 2004, **10**(20): 2483–2497
 28. Magierowski M, Jasnos K, Sliwowski Z, Surmiak M, Krzysiek-Maczka G, Ptak-Belowska A, Kwiecien S, Brzozowski T. Exogenous asymmetric dimethylarginine (ADMA) in pathogenesis of ischemia-reperfusion-induced gastric lesions: interaction with protective nitric oxide (NO) and calcitonin gene-related peptide (CGRP). *International Journal of Molecular Sciences*, 2014, **15**(3): 4946–4964
 29. Sanders K M, Ward S M. Nitric oxide and its role as a non-adrenergic, non-cholinergic inhibitory neurotransmitter in the gastrointestinal tract. *British Journal of Pharmacology*, 2019,

- 176(2): 212–227
30. Takahashi T. Pathophysiological significance of neuronal nitric oxide synthase in the gastrointestinal tract. *Journal of Gastroenterology*, 2003, **38**(5): 421–430
 31. Rivera L R, Pontell L, Cho H J, Castelucci P, Thacker M, Poole D P, Frugier T, Furness J B. Knock out of neuronal nitric oxide synthase exacerbates intestinal ischemia/reperfusion injury in mice. *Cell and Tissue Research*, 2012, **349**(2): 565–576
 32. Mazzoni M, Caremoli F, Cabanillas L, de Los Santos J, Million M, Larauche M, Clavenzani P, De Giorgio R, Sternini C. Quantitative analysis of enteric neurons containing choline acetyltransferase and nitric oxide synthase immunoreactivities in the submucosal and myenteric plexuses of the porcine colon. *Cell and Tissue Research*, 2021, **383**(2): 645–654
 33. Lefebvre R A. Nitric oxide in the peripheral nervous system. *Annals of Medicine*, 1995, **27**(3): 379–388
 34. Tappenbeck K, Hoppe S, Reichert C, Feige K, Huber K. *In vitro* effects of lidocaine on contractility of circular and longitudinal equine intestinal smooth muscle. *Veterinary Journal*, 2013, **198**(1): 170–175